

hours after transfection. COS-7 cells were incubated with EGF (0.1  $\mu\text{g/ml}$ ) [biotinylated, complexed to Texas Red-streptavidin (Molecular Probes, Eugene, OR)] in binding buffer [20 mM Hepes-NaOH (pH 7.5), 130 mM NaCl, and 0.1% bovine serum albumin] at 4°C for 60 min. Internalization of EGF was allowed by incubation in Dulbecco's modified

Eagle's medium at 37°C for 10 min, then excess EGF was removed with 0.2 M AcOH (pH 2.5) and 0.5 M NaCl at 4°C for 5 min. Cells were fixed in 3.7% formaldehyde, permeabilized with 0.2% Triton X-100, and immunostained with a polyclonal antibody to myc (Santa Cruz Biotechnology, Santa Cruz, CA) and fluorescein isothiocyanate-conju-

gated antibody to rabbit (Organon Teknica, Bostel, Netherlands). Internalization of EGF was observed by confocal microscopy (Bio-Rad).

37. We thank Y. Watanabe (Ehime University, Japan) for providing us with various synthetic phosphoinositides.

16 October 2000; accepted 15 December 2000

# Simultaneous Binding of PtdIns(4,5)P<sub>2</sub> and Clathrin by AP180 in the Nucleation of Clathrin Lattices on Membranes

Marijn G. J. Ford, Barbara M. F. Pearse, Matthew K. Higgins, Yvonne Vallis, David J. Owen, Adele Gibson,\* Colin R. Hopkins,\* Philip R. Evans,† Harvey T. McMahon†

Adaptor protein 180 (AP180) and its homolog, clathrin assembly lymphoid myeloid leukemia protein (CALM), are closely related proteins that play important roles in clathrin-mediated endocytosis. Here, we present the structure of the NH<sub>2</sub>-terminal domain of CALM bound to phosphatidylinositol-4,5-bisphosphate [PtdIns(4,5)P<sub>2</sub>] via a lysine-rich motif. This motif is found in other proteins predicted to have domains of similar structure (for example, Huntingtin interacting protein 1). The structure is in part similar to the epsin NH<sub>2</sub>-terminal (ENTH) domain, but epsin lacks the PtdIns(4,5)P<sub>2</sub>-binding site. Because AP180 could bind to PtdIns(4,5)P<sub>2</sub> and clathrin simultaneously, it may serve to tether clathrin to the membrane. This was shown by using purified components and a budding assay on preformed lipid monolayers. In the presence of AP180, clathrin lattices formed on the monolayer. When AP2 was also present, coated pits were formed.

Budding of clathrin-coated vesicles is a process by which cells package specific cargo into vesicles in a regulated fashion (1–3). Important functions are the uptake of nutrients, the regulation of receptor and transporter numbers on the plasma membrane, and the recycling of synaptic vesicles. AP180 and AP2 are both major components of clathrin coats. AP2 is a heterotetrameric complex that binds to phosphoinositides in the membrane and to the cytoplasmic domains of membrane proteins destined for internalization (1, 3, 4). AP2 binds clathrin and can stimulate clathrin cage assembly in vitro (5, 6). It also interacts with a range of cytoplasmic proteins including AP180 (7). Like AP2, AP180 also binds directly to clathrin and can stimulate clathrin cage assembly in vitro, limiting the size distribution of the resulting cages (8–11). The related proteins, CALM (AP180-2, a close homolog of synaptic AP180), LAP (the *Drosophila* AP180 homolog), and UNC-11 (the

*Caenorhabditis elegans* homolog), are all implicated in clathrin-coated vesicle endocytosis (12, 13). CALM was identified and named because of its homology to AP180 and to reflect its involvement in t(10;11) chromosomal translocations found in various leukemias (14). Disruptions of the *LAP* and *Unc-11* genes impair clathrin-dependent recycling of synaptic vesicles, resulting in fewer vesicles of more variable size. The NH<sub>2</sub>-terminal domain of AP180 (AP180-N) shows the highest degree of conservation across AP180 homologs, and binds to inositol polyphosphates (10, 15, 16), whereas the COOH-terminal domain contains the putative clathrin- and AP2-binding sites (Fig. 1A).

When expressed in COS-7 fibroblasts, both full-length AP180 and AP180-C (residues 530 to 915) inhibited uptake of epidermal growth factor (EGF) and transferrin (17) (Fig. 1B), as is the case for CALM (18). Clathrin was redistributed in transfected cells, and we noted fewer coated pits per unit of cell surface-membrane length (8% of control, Fig. 1C). This showed that endocytosis was inhibited by blocking clathrin-coated pit formation, consistent with the ability of the COOH-terminus to bind clathrin and to stimulate cage assembly in vitro (8–11). However, AP180-N overexpression did not inhibit EGF or transferrin uptake (Fig. 1B).

It had no apparent protein-binding partners but is more localized to the plasma membrane, consistent with binding to polyphosphoinositides (15, 16).

To probe the molecular basis of phosphoinositide interactions, we solved the structure of the NH<sub>2</sub>-terminal domain from the close AP180 homolog, CALM, at 2 Å resolution (19, 20) (crystals of AP180-N did not diffract well). There were nine  $\alpha$  helices forming a solenoid structure (Fig. 2). This is reminiscent of other protein families formed from a superhelix of  $\alpha$  helices such as the armadillo (21) and tetratricopeptide repeat (22) domains, but it is most similar to the ENTH domain of epsin (23) (Fig. 2B). The first seven helices of epsin superimposed well on those of CALM. In epsin, however, the final  $\alpha$ 8 helix folded back across the others, whereas in CALM the final three long helices continued the solenoidal pattern. Because of the high sequence homology of CALM-N and AP180-N (81% sequence identity) (Fig. 2), we can safely assume that the NH<sub>2</sub>-terminal domain of AP180 has the same structure.

X-ray data were collected at 2 Å resolution from CALM-N crystals soaked in a series of inositol phosphates and phospholipids. Binding was observed for inositol hexakisphosphate (D-myo-inositol-1,2,3,4,5,6-hexakisphosphate, InsP<sub>6</sub>), inositol-4,5-bisphosphate [Ins(4,5)P<sub>2</sub>], and a soluble short-chain (diC<sub>8</sub>) L- $\alpha$ -D-myo-phosphatidylinositol-4,5-bisphosphate. No significant binding was observed in the crystal for short-chain (diC<sub>8</sub>) L- $\alpha$ -D-myo-phosphatidylinositol-3,4,5-trisphosphate. The binding site is unusual (Fig. 2): Typical ligand-binding sites on proteins lie in a pocket or groove, but this site is on the surface, with the phosphates perched on the tips of the side chains of three lysines and a histidine, like a ball balanced on the fingertips. In all ligands, only the two phosphates were well ordered and contacted the protein. The cluster of lysines and histidine formed a marked positively charged patch on the surface (Fig. 2C), appropriate for a phosphate-binding protein.

Database searches with the AP180-N/CALM-N identified several classes of related sequences (Fig. 2H). First, there were the members of the AP180 family itself, with a conserved NH<sub>2</sub>-terminal domain, having PtdIns(4,5)P<sub>2</sub>-binding motifs, which we identified from the observed binding in the crystal, K(X)<sub>3</sub>KX(K/R)(H/Y). The COOH-terminal domains of these proteins contain clathrin-binding motifs (3, 24), as well as Asp-Pro-Phe (DPF)-like  $\alpha$ - and  $\beta$ -adaptin-

Medical Research Council (MRC) Laboratory of Molecular Biology, Hills Road, Cambridge, CB2 2QH, UK.

\*MRC Laboratory of Molecular and Cell Biology, University College London, Gower Street, London, WC1E 6BT, UK.

†To whom correspondence should be addressed. E-mail: pre@mrc-lmb.cam.ac.uk, hmm@mrc-lmb.cam.ac.uk

# REPORTS

binding motifs (7, 25) and Asn-Pro-Phe (NPF) motifs, which bind to Eps15 homology (EH) domains (26) (see Fig. 1A). Second, there were other proteins similar to AP180, containing the PtdIns(4,5)P<sub>2</sub>-binding motifs, but having unrelated COOH-terminal regions. Of these proteins, Huntingtin interacting protein 1 (HIP1) and SLA2p have actin-binding regions in their COOH-termini. Third, there were the epsin-related proteins; these showed a lower sequence homology in the NH<sub>2</sub>-terminus but shared the same structure for at least the first 140 residues (Fig. 2). They lack completely the PtdIns(4,5)P<sub>2</sub>-binding motif, but have a signature (D/E)PW motif in the loop connecting α1 to α2. According to our predictions, α-adaptin (which has no sequence homology to AP180) has a PtdIns(4,5)P<sub>2</sub>-binding motif near its NH<sub>2</sub>-terminus between the first two predicted helices. Indeed, a fragment from this region of the protein has been shown to bind PtdIns(4,5)P<sub>2</sub> (4).

Specificity of the phosphoinositide interaction with AP180-N and CALM-N was tested by sedimentation assays using liposomes or lipid tubules (19, 27, 28). Tubules containing 10% PtdIns(4,5)P<sub>2</sub> efficiently sedimented AP180-N and CALM-N with the same apparent affinity ( $K_M$  values of  $4.6 \pm 0.7 \mu\text{M}$  and  $5.8 \pm 1.7 \mu\text{M}$ , respectively) but mutations in the PtdIns(4,5)P<sub>2</sub> motif (KKK-EEE) abolished sedimentation (Fig. 3A). AP180-N was likewise sedimented with liposomes containing 10% PtdIns(4,5)P<sub>2</sub>, but not with liposomes when replaced with 10% phosphatidylserine (PtdSer), or 10% PtdIns, or 10% PtdIns(3,4)P<sub>2</sub> and less efficiently with liposomes containing 10% PtdIns(4)P or 10%

PtdIns(3,5)P<sub>2</sub> or 10% PtdIns(3,4,5)P<sub>3</sub> (Fig. 3B). Full-length AP180 binds to lipid tubules or liposomes containing PtdIns(4,5)P<sub>2</sub> with characteristics similar to those of AP180-N; however, a mutant in the PtdIns(4,5)P<sub>2</sub>-binding motif (KKK-EKE) does not (Fig. 3C).

Combinations of full-length AP180, AP2, and clathrin were then tested in sedimentation assays with PtdIns(4,5)P<sub>2</sub>-containing liposomes. AP2 was sedimented both in the presence and absence of AP180 (Fig. 3C). Clathrin only sedimented in the presence of AP180 [but not the PtdIns(4,5)P<sub>2</sub>-bind-

ing motif mutant], and then it associated preferentially with the lipid-bound AP180. Incubation of AP180, AP2, and clathrin resulted in the sedimentation of all components, and the clathrin in the pellet was resistant to 1% Triton X-100 treatment, implying a degree of polymerization (addition of Triton X-100 has been used as a purification step in the isolation of clathrin coats). Specificity of sedimentation was confirmed by using a number of controls including the absence of liposomes (Fig. 3C).

**Fig. 1.** Overexpression of AP180 in COS-7 cells inhibits endocytosis. (A) Domain structure of AP180 and other family members; red boxed regions (with annotated sequence identities) indicate the conserved domain homology. The strongest predicted clathrin-binding site is indicated (orange), but other sites are present, at least in AP180 and CALM. (B) Immunofluorescence data of EGF (green) uptake in cells transiently transfected with AP180, AP180-N, or AP180-C (stained red). The panel immediately below AP180-C is the same field stained for endogenous clathrin distribution (white). (C) Electron microscopy of immunogold-labeled transferrin receptors (arrows) in COS-7 cells transiently transfected with AP180-C. Transferrin receptors no longer accumulated in coated pits. WT, wild type.

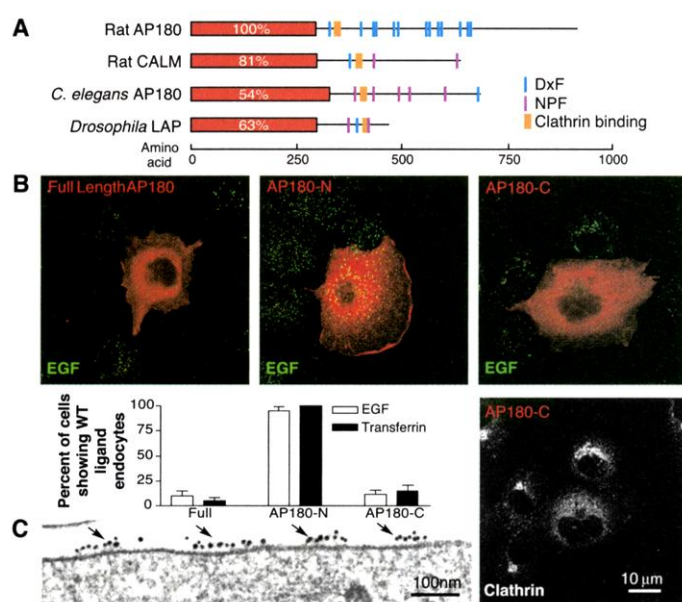


**Table 1.** Crystallographic statistics. Values in parentheses apply to the high-resolution shell.

	Native		EMTS		PtdIns(4,5)P <sub>2</sub>		Ins(4,5)P <sub>2</sub>		InsP <sub>6</sub>	
Data collection										
Resolution (Å) (outer bin)	2.0	(2.11)	2.0	(2.11)	2.0	(2.11)	2.0	(2.11)	2.0	(2.11)
R <sub>merge</sub> <sup>*</sup>	0.080	(1.036)	0.124	(2.03)	0.104	(1.153)	0.126	(1.958)	0.082	(0.952)
R <sub>meas</sub> <sup>†</sup>	0.083	(1.077)	0.145	(2.39)	0.112	(1.468)	0.136	(2.113)	0.088	(1.033)
Completeness (%)	100	(100)	100	(100)	100	(100)	99.4	(99.9)	100	(100)
Multiplicity	14.0	(13.3)	6.9	(6.7)	7.1	(7.0)	7.2	(7.0)	7.0	(6.4)
Wilson plot B (Å <sup>2</sup> )	43		43		43		43		44	
Refinement										
R (R <sub>free</sub> ) <sup>‡</sup>	0.187	(0.220)			0.195	(0.230)	0.193	(0.215)	0.190	(0.219)
⟨B⟩ (Å <sup>2</sup> )	48				49		49		49	
N <sub>reflections</sub> (N <sub>free</sub> )	26,057	(1,324)			26,014	(1,322)	25,847	(1,315)	25,815	(1,310)
N <sub>atoms</sub> (N <sub>water</sub> )	2,244	(130)			2,289	(128)	2,282	(128)	2,278	(128)
R <sub>msd</sub> bond length (Å)	0.031				0.032		0.026		0.031	
R <sub>msd</sub> bond angle (°)	2.1				2.5		2.2		2.4	
Number of Ramachandran violations	0		0		0		0			
MIR phasing										
Number of sites			EMTS							
			2 (one of them split)							
R <sub>deriv</sub> <sup>§</sup>			0.16							
R <sub>cullis</sub> <sup>  </sup> (centric, acentric)			0.63, 0.74							
Phasing power: isomorphous (anomalous) <sup>¶</sup>			1.35 (0.70)							
Mean figure of merit			0.59							
Figure of merit after solvent flattening (all data)			0.91*							

\* $R_{\text{merge}} = \sum_i |I_h - I_{h(i)}| / \sum_i I_h$ , where  $I_h$  is the mean intensity for reflection  $h$ .  $^\dagger R_{\text{meas}} = \sum_i \sqrt{(n/n-1)} |I_h - I_{h(i)}| / \sum_i I_h$ , the multiplicity weighted  $R_{\text{merge}}$ .  $^\ddagger R = \sum |F_o - F_{\text{calc}}| / \sum F_o$ .  $^\S R_{\text{deriv}} = \sum |F_{\text{PH}} - F_p| / \sum F_p$ .  $^\parallel R_{\text{cullis}} = \sum |F_{\text{PH}} - F_p| - |F_{\text{H(calc)}}| / \sum |F_{\text{PH}} - F_p|$ .  $^\P$  Phasing power =  $\langle |F_{\text{H(calc)}}| / \text{phase-integrated lack of closure} \rangle$ .

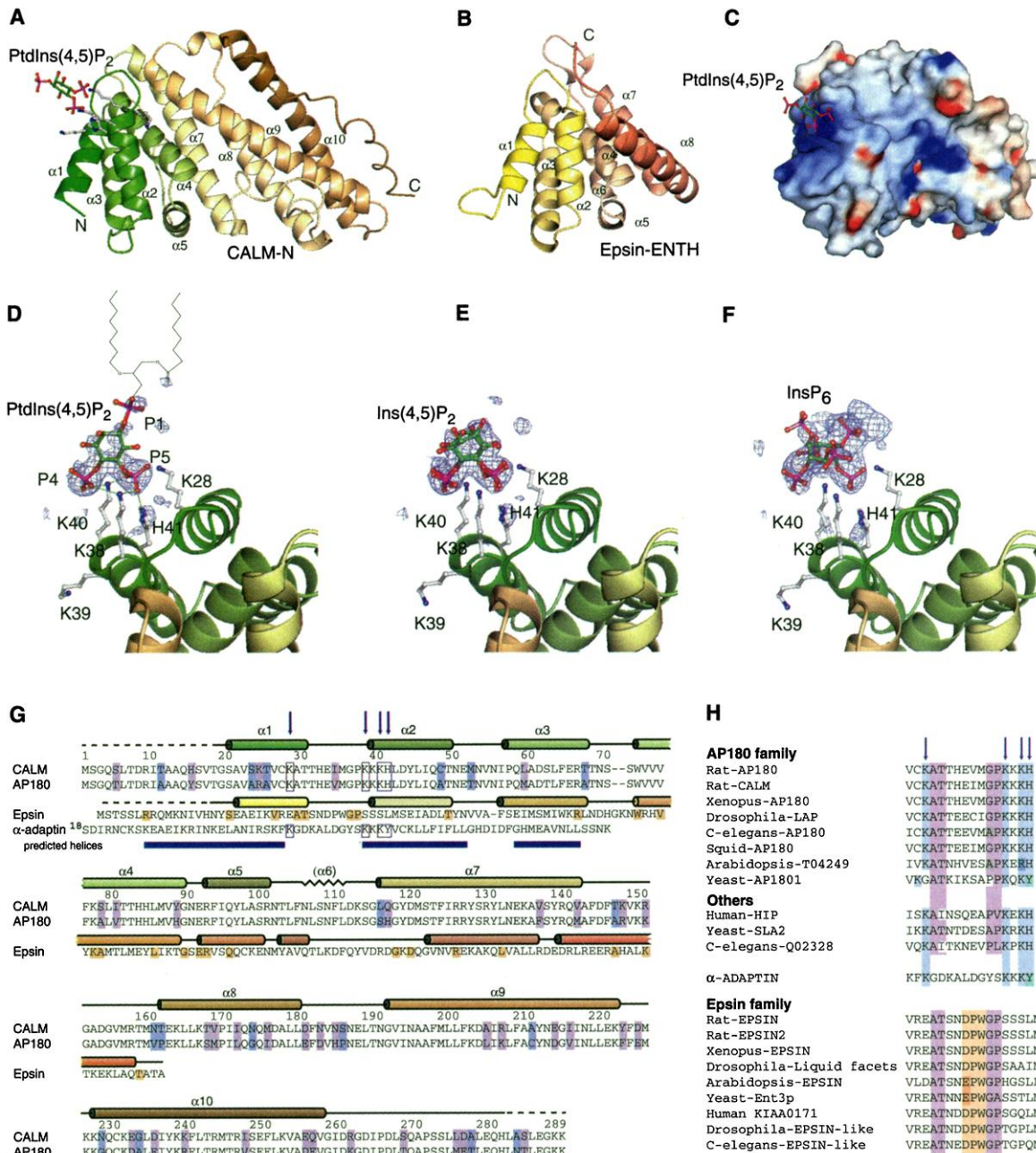
The recruitment of clathrin by AP180 was further investigated by electron microscopy to visualize clathrin lattice and cage formation. In the presence of AP180 and clathrin, latticelike structures formed on the surface of lipid monolayers (29) (Fig. 4A). Addition of AP2 resulted in the formation of more distinct electron-dense areas of clathrin assembly (Fig. 4B). Single-angle platinum shadowing of negatively stained grids showed that in the absence of AP2 the lattice was predominantly flat (Fig. 4C). Invaginated coated buds were

formed in the presence of AP2 (Fig. 4D). The diameter was well within the expected size range for brain-derived coated vesicles. In the absence of AP180, no detectable intermediates were visible by electron microscopy. When  $\text{PtdIns}(4,5)\text{P}_2$  was replaced by  $\text{PtdIns}$ , the flat clathrin lattices were no longer seen (Fig. 4E).

Our experiments demonstrate that the minimal requirements for the initial stage of coated pit invagination are clathrin, AP180, AP2, and  $\text{PtdIns}(4,5)\text{P}_2$ -containing membranes. However, with these compo-

nents, the pits do not invaginate completely, even in the presence of excess clathrin. AP180 concentrates clathrin on the membrane, and AP2s stimulate curved lattice assembly, consistent with their coat assembly activity (6). On a more general note, we show that the AP180  $\text{NH}_2$ -terminal domain is a  $\text{PtdIns}(4,5)\text{P}_2$ -binding domain responsible for membrane localization of AP180, and we propose that similar domains found in other proteins will also recruit them specifically to  $\text{PtdIns}(4,5)\text{P}_2$ -rich membranes.

**Fig. 2.** The structure of CALM-N bound to  $\text{PtdIns}(4,5)\text{P}_2$ . (A) Ribbon diagram of CALM-N, colored from green at the  $\text{NH}_2$ -terminus to gold at the  $\text{COOH}$ -terminus. (B) The ENTH domain of epsin in the same orientation [PDB code 1edu (23)]. (C) The surface of CALM-N colored by electrostatic potential, red +10  $\text{kT e}^{-1}$ , blue -10  $\text{kT e}^{-1}$ . This is a slightly different view from that in (A), to show the strong positive patch that binds  $\text{PtdIns}(4,5)\text{P}_2$ . (D) Close-up of  $\text{PtdIns}(4,5)\text{P}_2$ -binding site, showing a difference electron density map omitting the ligand, contoured at  $2\sigma$ . There was strong density only for the 4- and 5-phosphates, weak density for the inositol ring and the 1-phosphate, and none for the lipid chains. (E)  $\text{Ins}(4,5)\text{P}_2$  also shows most density for the phosphates; it was modeled as a 50:50 mixture of two binding modes interchanging the 4- and 5-phosphates. (F)  $\text{InsP}_6$  was probably bound in multiple orientations, and the orientation of the inositol ring was different from that of the bisphosphates. (G) Sequence alignments of the very similar CALM-N and AP180-N (81% identical, unshaded, further conserved residues shaded mauve), and the structurally similar epsin ENTH domain (16% sequence identity, shaded orange).  $\alpha$  Helices are shown as cylinders, colored as in A and B.  $\text{PtdIns}(4,5)\text{P}_2$ -binding residues are marked with arrows. Also shown is the  $\text{PtdIns}(4,5)\text{P}_2$ -binding region of  $\alpha$ -adaptin, with the conserved  $\text{PtdIns}(4,5)\text{P}_2$ -binding motif and predicted  $\alpha$  helices. (H) The  $\alpha 1$  to  $\alpha 2$  loop regions for three families of proteins:



AP180/CALM family with the  $\text{PtdIns}(4,5)\text{P}_2$ -binding motif (blue); some other proteins with the  $\text{PtdIns}(4,5)\text{P}_2$ -binding motif (blue); epsin family with the (D/E)PW motif (orange). Other conserved residues are colored purple. Yeast-SLA2 is Yeast-SLA2p.



**Fig. 3.** AP180-N binds, and has specificity for, PtdIns(4,5)P<sub>2</sub>. (A) AP180-N and CALM-N are sedimented by lipid tubules containing 10% PtdIns(4,5)P<sub>2</sub>. The measurements on the abscissa refer to the amount of PtdIns(4,5)P<sub>2</sub> in the experiment; the amount of tubules is therefore 10 times this value. Each assay contained 0.05 mg/ml protein. (B) Liposomes containing 10% cholesterol, 40% phosphatidylethanolamine, 40% phosphatidylcholine, and 10% of a test lipid were prepared and used to evaluate the lipid specificity of AP180-N. Each experiment contained 0.05 mg/ml protein and 50 μM of the lipid under investigation; each experiment, therefore, contained a total lipid concentration of 500 μM. (C) AP180 recruits clathrin to PtdIns(4,5)P<sub>2</sub> containing liposomes (27). Pellets (P) and supernatants (S) were separated by centrifugation. In AP180mut, lysines 38 and 40 were changed to glutamic acids. Although AP2 alone sedimented approximately as efficiently as AP180, it was not capable of sedimenting together with clathrin, possibly because of a requirement for cargo and/or oligomerization. Averages of at least three experiments are shown in the bar graph. Experiments contained 0.05 mg/ml AP180, 0.05 mg/ml AP2, 0.025 mg/ml clathrin in a final volume of 100 μl. All gels were stained with Coomassie Blue.

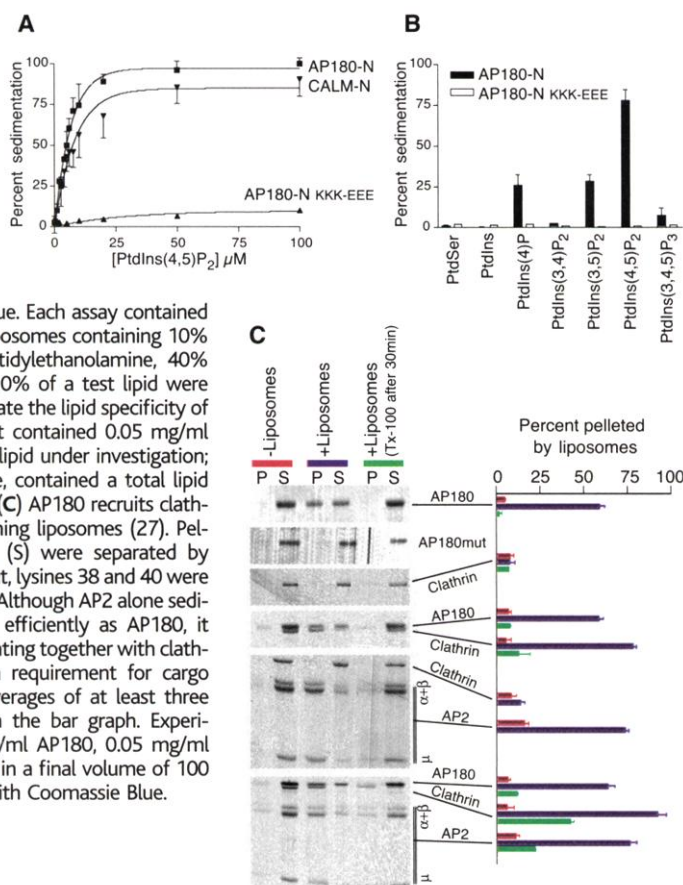
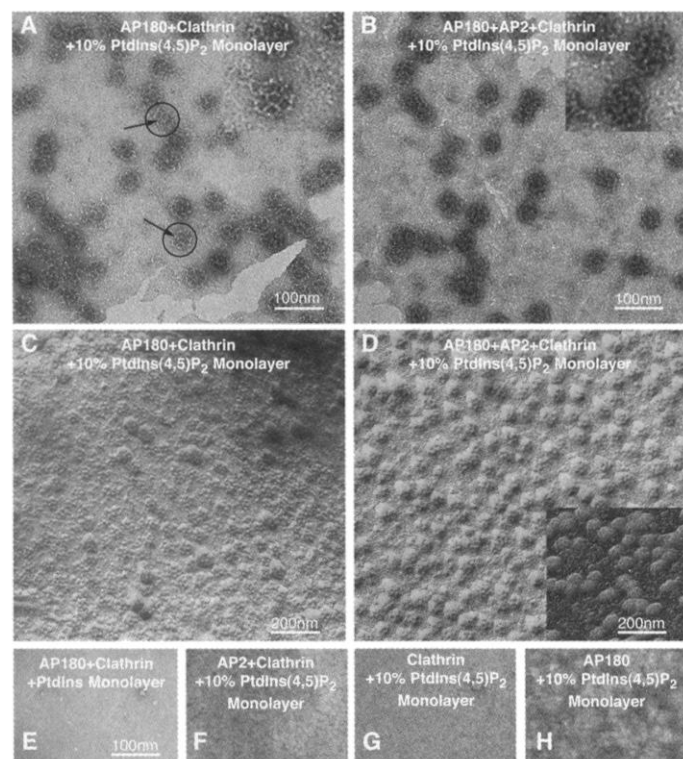


**Fig. 4.** Clathrin recruitment to lipid monolayers by AP180. (A) AP180, when incubated with clathrin in the presence of lipid monolayers recruited clathrin to the monolayer surface and promoted lattice assembly. The presence of a few pentagons among hexagons and the spherical outlines imply the beginning stages of coated pit invagination. The lattices formed had a diameter of 66 ± 7 nm. (B) The presence of AP180, AP2, and clathrin resulted in the formation of cages with electron-dense cores, which appeared deeply invaginated. The diameter of the cages thus formed was 77 ± 9 nm. Cracked areas lack cages. These experiments also worked on brain Folch lipids. (C and D) Single-angle platinum-shadowed monolayers showed that the clathrin assemblies were budded from the lipid surface in the presence of AP2 (inset: rotary platinum shadowing). We have shown more dense area of the grids compared with the negatively stained panels. (E to H) Controls showed no evidence of clathrin assemblies.



**Note added in proof:** It has been reported (44) that AP180 and its clathrin-binding domain inhibit transferrin endocytosis in HeLa and Cos cells and redistribute endogenous clathrin in HeLa cells.

# References and Notes

1. J. Hirst, M. S. Robinson, *Biochim. Biophys. Acta* **1404**, 173 (1998).
2. M. Marsh, H. T. McMahon, *Science* **285**, 215 (1999).
3. T. Kirchhausen, *Annu. Rev. Biochem.* **69**, 699 (2000).
4. I. Gaidarov, J. H. Keen, *J. Cell Biol.* **146**, 755 (1999).
5. T. Kirchhausen, *Annu. Rev. Cell Dev. Biol.* **15**, 705 (1999).
6. D. J. Owen, Y. Vallis, B. M. Pearse, H. T. McMahon, P. R. Evans, *EMBO J.* **19**, 4216 (2000).
7. The α and β appendage domains of the AP2 adaptor complex bind to cytoplasmic proteins with DPF-like motifs (Asp-Pro-Phe) (6, 30, 31). These proteins include AP180, amphiphysin, EPS15, epsin, and auxilin—all proteins known to function in clathrin-mediated endocytosis.
8. R. Lindner, E. Ungewickell, *J. Biol. Chem.* **267**, 16567 (1992).
9. S. A. Morris, S. Schroder, U. Plessmann, K. Weber, E. Ungewickell, *EMBO J.* **12**, 667 (1993).
10. W. Ye, N. Ali, M. E. Bembek, S. B. Shears, E. M. Lafer, *J. Biol. Chem.* **270**, 1564 (1995).
11. H. T. McMahon, *Curr. Biol.* **9**, R332 (1999).
12. B. Zhang et al., *Neuron* **21**, 1465 (1998).
13. M. L. Nonet et al., *Mol. Biol. Cell* **10**, 2343 (1999).
14. M. H. Dreyling et al., *Proc. Natl. Acad. Sci. U.S.A.* **93**, 4804 (1996).
15. F. A. Norris, E. Ungewickell, P. W. Majerus, *J. Biol. Chem.* **270**, 214 (1995).
16. W. Hao et al., *J. Biol. Chem.* **272**, 6393 (1997).
17. cDNAs encoding full-length AP180 and AP180-C (residues 530 to 915) were cloned into pCMV-MYC for expression in COS-7 cells. AP180-N (residues 1 to 289) was cloned into pcDNA. Clathrin-mediated endocytosis was measured by assaying EGF and transferrin uptake (32) on an MRC 1024 confocal microscope. Antibodies used for immunofluorescence are as follows: A14 (MYC-tag), Ra24 (AP180-N), and X-22 (clathrin), and secondary antibodies were conjugated with Texas Red or Cy-5. Transfected cells were compared with untransfected controls in their immediate vicinity. Blocked cells were defined as those transfected cells in which EGF or transferrin uptake was <20% that of untransfected controls. Blocked cells were expressed as a percentage of the total number of transfected cells, sampled in multiple fields and in multiple separate experiments. For immunoelectron microscopy of fibroblasts, cells either expressing the human transferrin receptor alone (cloned into pRK5), or coexpressing this with AP180-C were incubated at 4°C with B3/25 (antibody against human transferrin) conjugated to 10 nm gold for 90 min, rinsed, fixed, and processed as described (33). Sections were analyzed morphometrically by using standard techniques.
18. F. Tebar, S. K. Bohlander, A. Sorkin, *Mol. Biol. Cell* **10**, 2687 (1999).
19. AP180-N and CALM-N (residues 1 to 289) and mutants thereof were expressed as NH<sub>2</sub>-terminal glutathione S-transferase fusion proteins in BL21 cells. Protein was expressed overnight at 22°C and purified by passage over a glutathione-agarose column. The protein was cleaved with thrombin in 20 mM Hepes, pH 7.4, 150 mM NaCl, and 4 mM dithiothreitol (DTT). AP180-N and CALM-N were purified further by passage over Q-Sepharose followed by S200 gel filtration. For crystallization trials, AP180-N was concentrated to 40 mg/ml and CALM-N was concentrated to 16 mg/ml. For sedimentation assays, protein was typically used at 1 mg/ml. Full-length His<sub>6</sub>-tagged rat brain AP180 was purified from baculovirus-infected Sf9 cells 48 hours after infection. Protein was purified on a Ni-nitrilotriacetic acid (Ni-NTA) column, dialyzed into 20 mM Hepes, pH 7.4, 75 mM NaCl, and 4 mM DTT with protease inhibitors and bound to a Q-Sepharose column. Protein was eluted using a NaCl gradient from 75 to 300 mM.

- After concentration, the protein was passed through an S200 gel filtration column, using running buffer (20 mM Hepes, pH 7.4, 150 mM NaCl, 4 mM DTT). Clathrin and AP2 were purified from fresh pig brain as previously described (34). AP2 was dialyzed against 50 mM triethanolamine-KCl, pH 8.0, 200 mM NaCl, 0.2 mM EDTA, 0.1%  $\beta$ -mercaptoethanol, and 0.02%  $\text{NaN}_3$ . Clathrin cage formation was performed as described previously (6) in 25 mM Hepes, 125 mM K acetate, and 1 mM Mg acetate, pH 7.4.
20. Crystals of CALM-N (residues 1 to 289) were grown in seeded hanging drops against a reservoir containing 0.1 M Hepes, pH 7.5, 12 to 14% PEG 8000, and 8% ethylene glycol. They belong to space group  $P4_22_1$ , cell dimensions  $a = b = 77.93$  Å,  $c = 121.81$  Å, with one molecule per asymmetric unit. For the binding studies, crystals were soaked for 1 hour in 1 mM ligand in 0.1 M Hepes, pH 7.5, 14% PEG 8000, and 8% ethylene glycol. We were unable to find suitable conditions for cryoprotection, so all data sets were collected at room temperature from crystals mounted in capillaries, on beamline 9.6 at SRS Daresbury,  $\lambda = 0.88$  Å. By setting the ADSC Quantum 4 charge-coupled device detector to the fastest readout time ( $\sim 3$  s) and using a 3-s exposure for a  $1^\circ$  rotation, a  $90^\circ$  data set could be collected in less than 10 min with acceptable radiation damage. Images were integrated using Mosflm (35) and scaled using CCP4 programs (36). All data sets extended to 2 Å resolution and were reasonably strong to 2.1 Å resolution (see PDB depositions and Table 1 for details). Phases were derived from a single mercury derivative with two sites (crystals soaked for 1 hour in 1 mM ethylmercury thiosalicylate) by the program Sharp (37). Solvent flattening with Solomon led to an easily interpretable map. The model was built using O (38) and refined using Refmac5 (39). The termini (1 to 19 and 281 to 289) were not visible. Density was weak around the  $\alpha 7$  to  $\alpha 8$  loop (149 to 165); around the  $\alpha 9$  to  $\alpha 10$  loop (215 to 237); and the COOH-terminal region from about 267. Final  $R$  factors for the native and complexes were 0.187 to 0.195 ( $R_{\text{free}}$  0.215 to 0.230). Coordinates have been deposited in the PDB with access codes 1hf8 (native), 1hfa [PtdIns(4,5) $\text{P}_2$ ], 1hg2 [Ins(4,5) $\text{P}_2$ ], and 1hg5 [Ins $\text{P}_6$ ].
21. E. Conti, M. Uy, L. Leighton, G. Blobel, J. Kuriyan, *Cell* **94**, 193 (1998).
22. A. K. Das, P. W. Cohen, D. Barford, *EMBO J.* **17**, 1192 (1998).
23. J. Hyman, H. Chen, P. P. Di Fiore, P. De Camilli, A. T. Brunger, *J. Cell Biol.* **149**, 537 (2000).
24. E. C. Dell'Angelica, J. Klumperman, W. Stoerogel, J. S. Bonifacino, *Science* **280**, 431 (1998).
25. Single-letter abbreviations for the amino acid residues are as follows: A, Ala; C, Cys; D, Asp; E, Glu; F, Phe; G, Gly; H, His; I, Ile; K, Lys; L, Leu; M, Met; N, Asn; P, Pro; Q, Gln; R, Arg; S, Ser; T, Thr; V, Val; W, Trp; X, any amino acid; and Y, Tyr.
26. T. de Beer, R. E. Carter, K. E. Lobel-Rice, A. Sorkin, M. Overduin, *Science* **281**, 1357 (1998).
27. Lipid tubules [10% PtdIns(4,5) $\text{P}_2$ , 10% cholesterol, 40% phosphatidylcholine, 40% NFA-galactocerebrosides type II] were prepared as described in (40). Liposomes [10% PtdIns(4,5) $\text{P}_2$ , 10% PtdSer, 10% cholesterol, 35% phosphatidylcholine, and 35% phosphatidylethanolamine] were prepared by evaporating solvent from an appropriate mixture of lipids under a constant stream of argon. After resuspension in 10 mM Hepes, pH 7.4, the mixtures were extruded through a filter with pore size 0.1  $\mu\text{m}$ . Initially, tubules were used for comparison with our studies on dynamin, whose pleckstrin homology domain binds phosphoinositol head groups (40). Moreover, tubules are easier to sediment than liposomes. Dynamin was also used in the liposome experiments as a positive control for the incorporation of phosphatidyl inositols.
28. Protein(s) and liposomes or tubules (as appropriate) were added to reaction buffer (25 mM Hepes, pH 7.4, 125 mM K acetate, 1 mM Mg acetate) in a polycarbonate centrifuge tube (final volume of each experiment 50 or 100  $\mu\text{l}$ ). Experiments were incubated at room temperature for 30 min before sedimentation by centrifugation (78,000g for 20 min in a TLA100 rotor) and analyzed by Coomassie-stained gels. Densitometry was carried out using a Molecular Dynamics scanner and bands were integrated using ImageQuant for Macintosh v1.2.
29. A monolayer of lipid [same composition as 10% PtdIns(4,5) $\text{P}_2$  liposomes] was formed on the surface of a buffer droplet in a Teflon block (41), and the protein(s) of interest were introduced into the buffer. After 5 min, a carbon-coated gold electron microscopy grid was placed onto the monolayer. After 1 hour, the grid was removed and stained with uranyl acetate (2% uranyl acetate, 0.0025% polyacrylic acid). The technique has been used for the generation of two-dimensional crystals (41, 42) and, to our knowledge, has not been applied to study the formation of endocytic intermediates. Potassium in the buffer was critical for the efficient polymerization of clathrin in keeping with previous observations (43).
30. D. J. Owen et al., *Cell* **97**, 805 (1999).
31. L. M. Traub, M. A. Downs, J. L. Westrich, D. H. Fremont, *Proc. Natl. Acad. Sci. U.S.A.* **96**, 8907 (1999).
32. P. Wigge, Y. Vallis, H. T. McMahon, *Curr. Biol.* **7**, 554 (1997).
33. C. E. Futter, A. Pearce, L. J. Hewlett, C. R. Hopkins, *J. Cell Biol.* **132**, 1011 (1996).
34. C. J. Smith, N. Grigorieff, B. M. Pearce, *EMBO J.* **17**, 4943 (1998).
35. A. G. W. Leslie, in *Joint CCP4 and ESF-EACMB Newsletter on Protein Crystallography* No. 26 (SERC, Daresbury Laboratory, Warrington, UK, 1992).
36. Collaborative Computational Project No. 4, *Acta Crystallogr.* **D50**, 760 (1994).
37. E. de la Fortelle, G. Bricogne, *Methods Enzymol.* **276**, 472 (1997).
38. T. A. Jones, J. Y. Zou, S. W. Cowan, M. Kjeldgaard, *Acta Crystallogr.* **A47**, 110 (1991).
39. G. N. Murshudov, A. A. Vagin, E. J. Dodson, *Acta Crystallogr.* **D53**, 240 (1997).
40. M. H. Stowell, B. Marks, P. Wigge, H. T. McMahon, *Nature Cell Biol.* **1**, 27 (1999).
41. D. Levy et al., *J. Struct. Biol.* **127**, 44 (1999).
42. R. D. Kornberg, S. D. Darst, *Curr. Opin. Struct. Biol.* **1**, 642 (1991).
43. J. E. Heuser, R. G. Anderson, *J. Cell Biol.* **108**, 389 (1989).
44. X. Zhao et al., *J. Cell Sci.* **114**, 353 (2001).
45. We thank O. Perisic for advice on liposome preparation, E. Ungewickell for the AP180 clone, L. Serpell and J. Berriman for assistance with platinum shadowing, D. Brodersen and B. Clemons for assistance with data collection, and the staff of beamline 9.6, SRS Daresbury. Also, we thank N. Unwin and members of our labs for extensive discussion.

20 November 2000; accepted 18 December 2000

# Notch Inhibition of RAS Signaling Through MAP Kinase Phosphatase LIP-1 During *C. elegans* Vulval Development

Thomas Berset, Erika Fröhli Hoier, Gopal Battu, Stefano Canevascini, Alex Hajnal\*

During *Caenorhabditis elegans* vulval development, a signal from the anchor cell stimulates the RTK/RAS/MAPK (receptor tyrosine kinase/RAS/mitogen-activated protein kinase) signaling pathway in the closest vulval precursor cell P6.p to induce the primary fate. A lateral signal from P6.p then activates the Notch signaling pathway in the neighboring cells P5.p and P7.p to prevent them from adopting the primary fate and to specify the secondary fate. The MAP kinase phosphatase LIP-1 mediates this lateral inhibition of the primary fate. LIN-12/NOTCH up-regulates *lip-1* transcription in P5.p and P7.p where LIP-1 inactivates the MAP kinase to inhibit primary fate specification. LIP-1 thus links the two signaling pathways to generate a pattern.

MAP kinase phosphatases (MKPs) belong to the family of dual-specificity phosphatases that inactivate different types of MAP kinases by dephosphorylating the critical phosphotyrosine and phosphothreonine residues of the kinases (1). The transcription

of MKPs is rapidly induced by various stimuli such as growth factors and cellular stresses that activate MAP kinases, suggesting that MKPs may participate in an autoinhibitory feedback loop.

To study the role of MKPs in RTK/RAS/MAPK signaling during development, we searched the *C. elegans* genome sequence for homologs of vertebrate MKPs. Among the 185 predicted phosphatases, we identified a candidate, termed *lip-1* (lateral signal induced phosphatase-1, open read-

Division of Cancer Research, Department of Pathology, University of Zürich, Schmelzbergstrasse 12, CH-8091 Zürich, Switzerland.

\*To whom correspondence should be addressed. E-mail: ahajnal@pathol.unizh.ch